A magnetic x-ray diffraction investigation of gadolinium selenide

1996 J. Phys.: Condens. Matter 8 2425

(http://iopscience.iop.org/0953-8984/8/14/016)

J. Phys.: Condens. Matter **8** (1996) 2425–2435. Printed in the UK

A magnetic x-ray diffraction investigation of gadolinium selenide

M M R Costa†, M J M de Almeida†, W J Nuttall‡, W G Stirling‡, C C Tang§, J B Forsyth‖ and M J Cooper¶

† Departamento de Fisica, Universidade de Coimbra, P-3000 Coimbra, Portugal
‡ Department of Physics, Keele University, Keele, Staffs ST5 5BG, UK
§ Daresbury Laboratory, Warrington, Cheshire WA4 4AD, UK
‖ Rutherford Appleton Laboratory, Chilton, Oxon OX11 0QX, UK
¶ Department of Physics, University of Warwick, Coventry CV4 7AL, UK

Received 8 September 1995, in final form 18 January 1996

Abstract. A single-crystal synchrotron radiation study of gadolinium selenide has been made in the temperature range 15–100 K. GdSe has the rocksalt structure and becomes antiferromagnetic below a reported Néel temperature of 65 K. At 15 K, magnetic reflections are observed at $\boldsymbol{G}+\boldsymbol{\tau}$ with modulation wavevector $\boldsymbol{\tau} = \{1/2, 1/2, 1/2\}$ propagating from reciprocal lattice point $\boldsymbol{G}$. This is achieved by exploiting the resonant enhancement in the vicinity of the Gd L_{II} and L_{III} edges. Similar enhancements are observed at the two edges, with the maximum effect occurring approximately 3 eV above the absorption edge. The temperature dependence of the intensity of the magnetic reflections indicates a Néel temperature of 63(1) K. These measurements, together with high-resolution studies of the fundamental reflections ($\boldsymbol{\tau} = \mathbf{0}$), contribute further evidence of magnetic or structural changes in the sample at 37(1) K. Our observations are discussed and compared with previous x-ray diffraction and magnetic susceptibility measurements.

1. Introduction

During the last ten years the study of lanthanide and actinide antiferromagnetism has been reinvigorated and advanced through the use of synchrotron x-ray techniques. In particular, the tunability of the source has enabled magnetic diffraction experiments to be performed near the absorption edges of constituent atoms where x-ray resonant exchange scattering (XRES) enhances the intensity of magnetic scattering. This effect, first observed for nickel [1], has revolutionized experimental studies of the magnetic structure of 4f and 5f antiferromagnets where particularly large enhancements of the diffraction signals are observed at L and M edges. The first systematic reports of such behaviour were made by Gibbs and co-workers [2].

Gadolinium compounds are of particular interest for study using resonant x-ray techniques. First, the extremely large thermal neutron cross section for naturally occurring gadolinium (29 400 barns at $\lambda = 1.8$ Å) has severely limited the number of neutron scattering investigations. Second, gadolinium is of special interest in consolidating our understanding of the maturing XRES spectroscopy. This is a consequence of the element's position midway across the 4f series and the fact that in both its bound and free atom states the 4f orbital is exactly half filled. As such it is of great interest in assessing the systematics of the resonant spectroscopic properties. In particular the 'branching ratio' given by the

0953-8984/96/142425+11$19.50

relative intensities of the L_{III}/L_{II} enhancements has recently been tabulated for the 4f series [3] and has been the subject of recent discussion in the literature [3, 4]. To our knowledge x-ray diffraction studies of magnetism in elemental gadolinium have thus far not been undertaken by any group. This is a consequence of the metal's ferromagnetic ordering (the Curie point being just above room temperature) which would give rise to magnetic diffraction peaks superimposed on the far brighter charge scattering. Antiferromagnetic (AF) gadolinium compounds are not subject to this constraint as the different lattice periodicity and/or symmetry for the magnetic structure leads to additional distinct diffraction peaks solely associated with the magnetism.

We are aware of two other magnetic x-ray scattering studies of gadolinium AF compounds. The first is that due to Vettier *et al* in which the modulation of the magnetic moment in a gadolinium–yttrium multilayer was investigated using both synchrotron and rotating anode sources [5]. The second more recent study is that of Detlefs and coworkers [6]. This latter study uses XRES to investigate the relationship between the magnetic state of the gadolinium ions in $GdNi_2B_2C$ and the observed superconductivity of various rare-earth nickel boride carbides.

In this paper we discuss the magnetic and structural properties of the rocksalt structure antiferromagnet GdSe. This compound is especially suitable for advancing our understanding of XRES and gadolinium magnetism owing to its high degree of chemical stability, the availability of high-quality single crystals and an existing literature on this material.

One neutron powder experiment has been performed on a suspension of GdSe particles in a powdered copper matrix [7]. At 4.2 K magnetic peaks were observed at d-spacings corresponding to a magnetic propagation vector $\boldsymbol{q} = \{1/2, 1/2, 1/2\}$. The diffraction pattern is compatible with f.c.c. type II antiferromagnetic ordering, and the magnetic moments of Gd^{3+} were said to lie within the {111} planes. The Néel temperature, T_N, obtained from low-temperature magnetic susceptibility measurements was estimated by these authors to be 60 K. Additional insight into the magnetic structures of GdSe has been provided by low-temperature x-ray studies of its lattice distortions and measurements of its magnetic susceptibility [8]. Hulliger and Siegrist report that six samples were examined and describe their chemical compositions as analysed by electron beam microanalysis [8]. One sample, $Gd_{0.93(2)}Se_{1.07(2)}$, was deficient in gadolinium, was believed to contain oxygen and had a significantly smaller lattice parameter $a = 5.7784(6)$ Å at 22 °C than the remainder which were, if anything, poor in selenium. The latter had compositions $Gd_{1-x}Se_{1+x}$ with x between $-0.001(20)$ and $-0.015(20)$ and lattice parameters, determined using powdered material, in the range 5.7803–5.7876(6) Å. The magnetic susceptibility measurements were made on these samples as powder and as oriented single crystals with the magnetic field oriented parallel to ⟨111⟩ or ⟨100⟩ and showed Néel temperatures in the range 58–65(2) K. Below a T_N of 65(2) K, three approximately stoichiometric samples showed that the alignment of the magnetic moments along ⟨111⟩ is accompanied by a rhombohedral elongation along this direction leading to a trigonal structure assumed to be of antiferromagnetic type II (phase I). At temperatures between 39.5 and 34 K these crystals distorted to a monoclinic phase as the spins flipped to become parallel to original cubic ⟨110⟩ directions (phase II). However a fourth sample, within the same range of stoichiometry but with a lower T_N of 58 K, exhibited quite a different behaviour, an immediate transition to a structure having a pseudo-rhombohedral compression of the f.c.c. unit cell and a true symmetry which may be monoclinic (phase III). This phase, in which the spins were reported to lie within the (111) planes, persisted down to 4.2 K. An analysis based upon a high-temperature Curie–Weiss approximation has estimated the effective magnetic moment to be approximately $8\mu_B$ [8],

in agreement within estimated error with the calculated value of $g[J(J+1)]^{1/2}$.

It is clear from the work of Hulliger and Siegrist that sample stoichiometry is a vital consideration in assessing the magnetic and structural properties of gadolinium selenides. It will be of great interest to see if this strict requirement is characteristic of rare-earth selenides generally and we shall be conscious of this in our planned studies of terbium selenide. In order to assess the precise stoichiometry of our sample we have performed an energy dispersive x-ray (EDX) spectroscopic study of the emitted fluorescence from the sample when scanned in a JEOL 100 CX electron microscope. By considering the intensities of the Gd $L_{\alpha 1,2}$ and $L_{\beta 1}$ and Se $Ka_{\alpha 1,2}$ fluorescence lines emitted by the sample and reference samples of elemental gadolinium and selenium we may infer the relative proportions of the two elements in our sample. We have also been able to confirm the absence of any heavy impurities in the sample studied. By comparing the ratios of measured gadolinium and selenium peak intensities we obtain the following estimate of the sample stoichiometry: $Gd_{0.969}Se_{1.031}$. Estimating the random errors associated with this measurement of $Gd_{1-x}Se_{1+x}$ we obtain $x = 0.031 \pm 0.003$. Some caution is advised in respect of this result as the quoted error takes no account of systematic effects which despite our care may still be present in the data.

In order to provide a second quantitative description of the chemical state of our sample we have made quantitative measurements of the colour of our sample as this is known to correlate strongly with sample composition [8]. Ten separate quantitative measurements have been made of the tristimulus specification of our sample's colour at different points on its surface. Measurements were made in a standard configuration of 45° illumination and surface normal measurement (45/0 geometry). The instrument used was the Minolta Chroma Meter CR-241, which is a three-filter instrument particularly suited for studies of small samples. The results obtained are expressed in the international standard (CIELAB 1976) colour space using D65 illuminant (artificial daylight). The quantitative results averaged over the whole sample are lightness $= 4.78 \pm 3.72$; chroma $= 3.98 \pm 2.22$ and hue $= 72.84^\circ \pm 6.49^\circ$. Of greatest interest is the hue measurement which is expressed using an angular scale where 0° corresponds to red and 90° corresponds to yellow. As such we are able to say that the colour of our GdSe single crystal is clearly more yellow than red. We expect that the hue value obtained represents a precise indicator of the stoichiometry of our small single-crystal sample, which may be compared with measurements from other GdSe samples. With reference to table 1 of [8] we note that the sample colour measurements of our sample imply near 1:1 stoichiometry with little indication of oxidation. It is possible that our sample may be closer to 1:1 stoichiometry than the EDX measurements imply. The relatively large error in the quoted value of hue reflects variations within the ten separate measurements across the surface of our small single-crystal sample. From this we infer that the sample studied has some range of stoichiometries across its surface.

2. Experimental details

The measurements were made on the seven-circle diffractometer at station 9.4 of the Synchrotron Radiation Source (SRS) at Daresbury Laboratory, UK. This station receives hard x-ray synchrotron radiation from a three-pole 5 T superconducting wiggler magnet. The polychromatic radiation from the wiggler is first focused by a platinum-coated, toroidal mirror and then monochromatized using a channel-cut, double-bounce Si(111) crystal. The diffractometer has a vertical scattering plane. The incident beam was collimated by three sets of slits to produce a beam area of approximately 1×3 mm^2 at the sample. An ionization chamber located at the end of the beamline was used to monitor the incident beam intensity.

In order to minimize the effect of air scattering, the incoming and outgoing flight-paths were filled with helium. Further slits were used at both ends of the outgoing flight-path to define an aperture in front of the solid-state detector and to minimize the background scattering.

The GdSe single crystal used in our study has approximate dimensions $3 \times 2 \times 1$ mm^3 and has the near-1:1 stoichiometry discussed earlier. Preliminary Laue photographs were taken to confirm that a $\langle 001 \rangle$ direction is perpendicular to the largest face. The crystal was mounted on the cold finger of a closed-cycle helium refrigerator (operating over a temperature range of 15–300 K) with [110] approximately parallel to the horizontal θ axis of the diffractometer and its orientation matrix determined from by centring the (002), (004), $(\bar{2}\bar{2}4)$ and $(-2\,-2\,4)$ reflections. The mosaic spread was 0.07° (FWHM), as derived from the widths of transverse (θ) scans of (224) and (004).

The energy calibration of the monochromator was determined from measurements of the fluorescence at the L_{II} (7930 eV) and L_{III} (7243 eV) absorption edges of gadolinium. Once calibrated, the incoming photon beam could be reliably tuned in energy through the gadolinium resonances in order to observe the magnetic reflections.

3. Results

3.1. Magnetic structure

The resonant magnetic x-ray scattering cross section is the subject of active discussion in the literature. The initial theoretical description of these processes used a formalism based upon vector spherical harmonics [9]. It is only recently that the resonant cross section has been formulated in a vector space characteristic of actual scattering experiments [10]. As such this description mirrors the discussions of non-resonant magnetic x-ray scattering in the literature [11, 12]. The resonant cross section has two principal excitation dependences, the dipolar ($E1$) and the quadrupolar ($E2$) each of which has a hierarchy of terms. The full cross section may be broken down to being approximately [10]

$$f_n = [(\varepsilon' \cdot \varepsilon)F^{(0)} - \mathrm{i}(\varepsilon' \times \varepsilon) \cdot \boldsymbol{z}_n F^{(1)} + (\varepsilon' \cdot \boldsymbol{z}_n)(\varepsilon \cdot \boldsymbol{z}_n)F^{(2)}]_{E1} + [(\boldsymbol{k}' \cdot \boldsymbol{k})(\varepsilon' \cdot \varepsilon)F^{(0)} - \mathrm{i}[(\boldsymbol{k}' \cdot \boldsymbol{k})(\varepsilon' \times \varepsilon) \cdot \boldsymbol{z}_n + (\varepsilon' \cdot \varepsilon)(\boldsymbol{k}' \times \boldsymbol{k}) \cdot \boldsymbol{z}_n]F^{(1)}]_{E2}$$

where ε and ε' are unit vectors describing respectively the incoming and outgoing x-ray polarization. Similarly $\boldsymbol{k}$ and $\boldsymbol{k}'$ are the incoming and outgoing photon momenta while the unit vector $\boldsymbol{z}_n$ describes the spin moment at site n. The terms $F_{E1}^{(j)}$ and $F_{E2}^{(j)}$ are in each case the appropriate operator composed of a linear combination of matrix elements describing quantum-mechanically allowed electronic transitions. The first dipolar term above is associated with normal Thompson charge scattering and is effectively independent of the magnetism. The second dipolar term, scaled by $(\varepsilon' \times \varepsilon) \cdot \boldsymbol{z}_n$, predominates both theoretically and experimentally over both higher-order dipolar terms and all quadrupolar terms [13]. It is interesting to note that this term is only of non-zero magnitude when the plane of polarization is rotated in the scattering process and when the direction of the outgoing photon, given by $(\varepsilon' \times \varepsilon)$, is not perpendicular to the magnetization. Therefore XRES experiments may be able to not only provide an insight into the periodicities of the magnetic lattice but also give information concerning the individual spin directions. These ideas have been discussed by Tang and coworkers [14] and are reminiscent of the stronger geometric constraints on the cross section which are often employed usefully in magnetic neutron diffraction [15].

The orientation of our sample and the limited degrees of freedom for crystal movement restricted the study to in-plane (hhl) type reflections. In addition restrictions arose from the

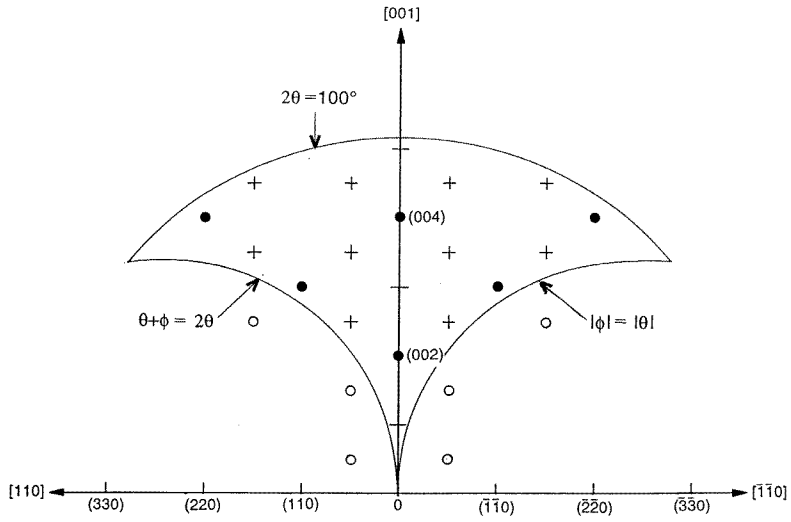

Figure 1. A schematic representation of the various diffraction peaks accessible in the (*hhl*) scattering plane. The filled circles denote the charge peaks from the crystalline lattice. The crosses denote magnetic reflections of the type $\boldsymbol{G}+\boldsymbol{\tau}$ with $\boldsymbol{\tau}=\{1/2,1/2,1/2\}$. The open circles denote inaccessible magnetic peaks. The lines represent the different geometric limits imposed by the reflection geometry.

need to maintain the sample in (001)-face reflection geometry. Figure 1 shows the portion of reciprocal space for the GdSe f.c.c. structure which was accessible in the geometry of the experiment. Magnetic reflections of the type $\boldsymbol{G}+\boldsymbol{q}$ with $\boldsymbol{q}=\{1/2,1/2,1/2\}$ are expected to occur from the antiferromagnetic ordering inferred from a neutron diffraction study [7]. The sample was cooled to 20 K and several longitudinal (θ–2θ) scans were made through each reciprocal lattice point shown in figure 1 at an energy close to the L_{III} absorption edge. The expected magnetic satellites at $(1/2,1/2,5/2)$, $(1/2,1/2,7/2)$, $(1/2,1/2,9/2)$, and $(3/2,3/2,9/2)$ were observed. At the remaining accessible reciprocal lattice points the satellite peak intensity was found to be too small to be measured with satisfactory statistical accuracy within the time available for the experiment. Figure 2 shows a typical θ–2θ scan through the $(1/2,1/2,7/2)$ magnetic peak at 20 K. Similar measurements were carried out at 45 K and the relative intensities of the observed magnetic peaks were found to be similar at the two temperatures. Further measurements at the L_{II} resonant energy again confirmed the presence of the same magnetic satellites. Second-order satellites of modulation wavevector $2\boldsymbol{q}$ are predicted and have been observed in several 4f AF systems [16]. In our studies we were particularly curious as to whether magnetic diffraction might arise at such positions as a consequence of the magnetic spin structure. We expect the $2\boldsymbol{q}$ satellites to have a modulation wave vector $\boldsymbol{\tau}=2\boldsymbol{q}=\{111\}$ propagating from any reciprocal lattice point, $\boldsymbol{G}$. In this way we might expect $2\boldsymbol{q}$ satellites to be visible at the (001), (003), and (114) charge-forbidden lattice points (among others). The (114) satellite would, for instance, represent $2\boldsymbol{q}$ propagations from the (003) and (225) reciprocal lattice points. We checked exhaustively for $2\boldsymbol{q}$ satellites at the three positions mentioned above. X-rays tuned to both the L_{II} and L_{III} absorption edges were used for studies at various temperatures in the ordered phase. No such satellites were observed. The absence of these higher-order satellites is entirely consistent with the expected behaviour of the MnO (type

II) AF ordering suggested by McGuire and coworkers from their neutron diffraction study [7].

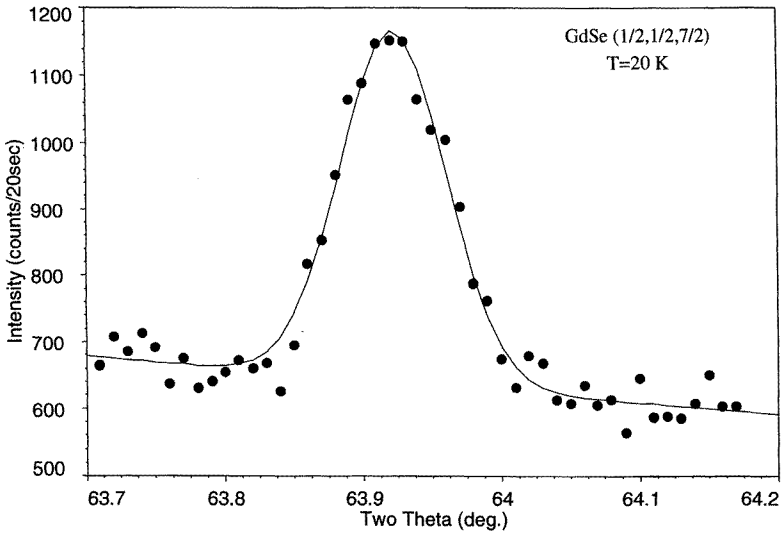

Figure 2. Representative resonant magnetic diffraction data at the $(1/2, 1/2, 7/2)$ position at 20 K. The data shown were obtained from a longitudinal (θ–2θ) scan at the L_{III} edge (7.243 keV).

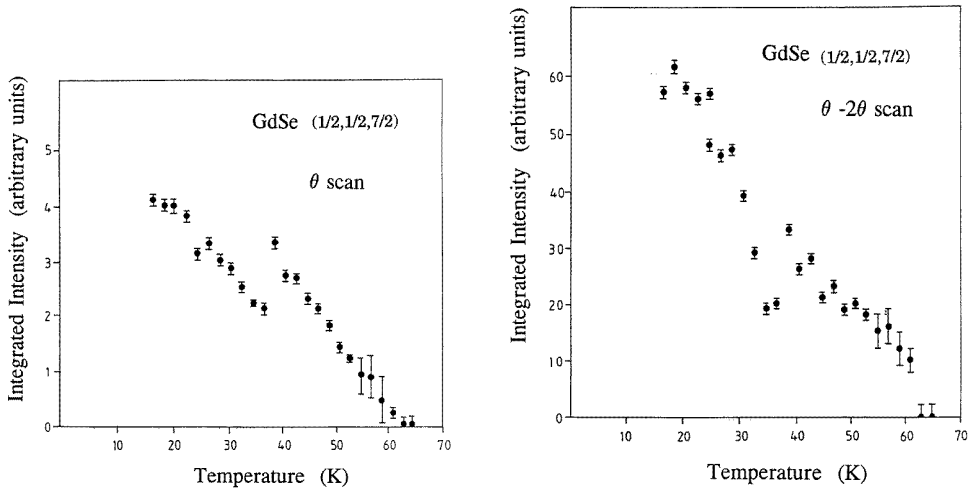

Figure 3. Right, the integrated intensity of the $(1/2, 1/2, 7/2)$ magnetic peak as a function of temperature, extracted from longitudinal (θ–2θ) scans; left, equivalent data from transverse (θ) scans through the $(1/2, 1/2, 7/2)$ peak. Note in each case the dip in the measured intensity at approximately 37 K.

The variation of the intensity of the $(1/2, 1/2, 7/2)$ peak was also investigated as a function of temperature. The integrated intensity of this reflection was measured at each temperature in sequential θ–2θ and θ scans. Before each measurement the temperature

of the sample was stabilized to within ±0.2 K. The results are shown in figure 3. The integrated intensity decreases to almost zero in the vicinity of the Néel temperature at 63(1) K. However, a small residual intensity could still be measured at temperatures well above T_N. An interesting feature of the temperature variation below T_N is the pronounced reduction in intensity which occurs at 37(1) K. We associate this reduction with the phase transition to the monoclinic phase II reported to occur in the range 34–39.5 K in the majority of GdSe samples examined in [8], but it could be produced by a spin reorientation to the [110] direction. The prospects for further x-ray single-crystal investigations of this transition are somewhat limited; this is largely a consequence of the geometrical constraints placed upon the experiment by the need to use a reflection condition. Further insights into the interesting behaviour of this material might be provided by magnetic x-ray powder diffraction, muon spin relaxation, and high-energy neutron diffraction although none of these experiments would be straightforward to perform or interpret.

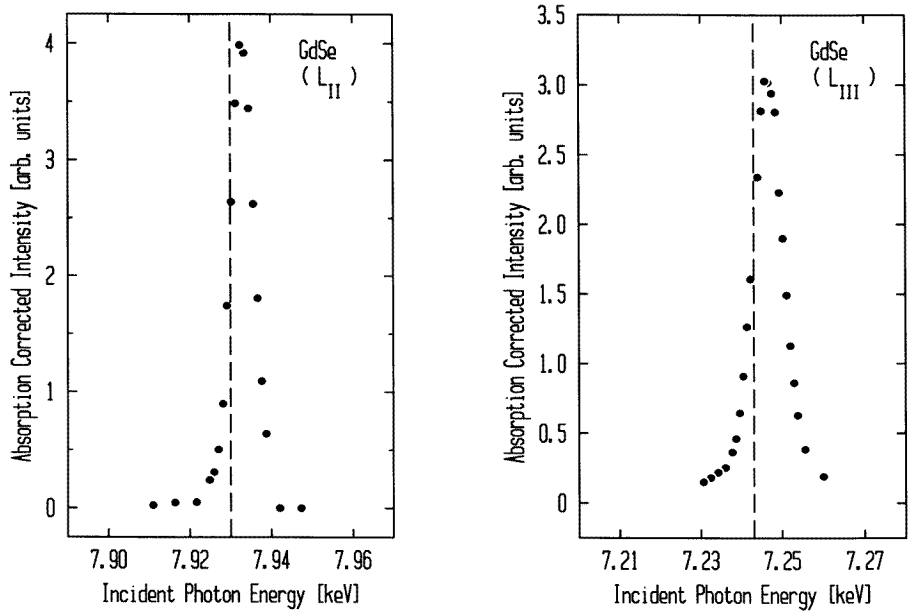

Figure 4. The energy dependence of the integrated intensity of the $(1/2, 1/2, 7/2)$ magnetic reflection at 32 K; the L_{III} and L_{II} absorption edges are marked by dashed lines. The data have been corrected for absorption. Appropriate error bars are smaller than the points shown.

3.2. Resonant exchange scattering

XRES spectra are of inherent interest because they provide information on the electronic structure of the Gd ion through their peak positions with respect to the absorption edges and through the measured branching ratio (the ratio of the L_{III} to L_{II} x-ray emission amplitudes). The intensity of the $(1/2, 1/2, 7/2)$ magnetic satellite, as a function of energy in the vicinity of the L_{II} and L_{III} edges, is shown in figure 4. These data have been corrected for the gadolinium absorption factor μ, which also shows a strong energy dependence in the vicinity of the L_{II} and L_{III} edges.

Variations in the sample absorption affect the x-ray penetration depth, the illuminated volume, and the ability of the diffracted x-ray to leave the sample. The absorption corrections are therefore important, so a direct measurement of the energy-dependent absorption coefficient of gadolinium was made using a 5 μm foil. An NaI scintillation detector, selected for its flat response over a wide range of photon energies, was used to measure the transmitted photon flux. The incident beam was tightly collimated to avoid saturating the detector and an ionization chamber was used to monitor its intensity at each energy. Detector readings were recorded with and without the foil at energies ranging from above that of the L_{III} edge to below the L_{II} edge. The magnitude of the magnetic enhancement at the L_{II} and L_{III} edges is similar, leading to an intensity ratio of 1.3:1 (N.B. the ratio in the uncorrected raw data is 1.6:1). The maximum enhancement of the magnetic intensity was observed to occur approximately 3 eV above both the L_{III} edge and the L_{II} edge. A similar shift of the maximum intensity to an energy slightly above that of the L_{III} edge has been reported to occur in other rare earth materials [17–21]. Hannon and coworkers [9] have explained such shifts in terms of a combination of electric dipole and quadrupole transitions between the 2p and 5d or 4f magnetic states, respectively.

3.3. Structural (charge scattering) studies

Structural studies have been performed to obtain further information about the phase transitions that accompany the evolution of magnetic order in GdSe. Good longitudinal wavevector resolution was achieved by employing a Si(111) analyser on the 2θ arm of the diffractometer. Longitudinal and transverse scans of the (002) and (004) reflections were made sequentially at different stabilized temperatures in the range 15–100 K. Analysis of the longitudinal scans enabled the temperature dependence of the lattice parameter to be determined as shown in figure 5. There appear to be three distinct regions as shown by the lines: below approximately 30 K the lattice parameter is independent of temperature. Above about 45 K the lattice expands linearly with temperature. Between approximately 30 K and 45 K an intermediate regime is observed. Figure 6 illustrates the changing width of these reflections; there is a minimum in the width at approximately 40 K, which possibly corresponds to a longer-range real-space translational periodicity. Figure 7 shows transverse θ scans through the (002) reflection. A significant change in the mosaicity is observed both in the vicinity of the Néel temperature and near 40 K.

4. Conclusions

The use of the resonant magnetic scattering technique is especially useful for gadolinium compounds, given the extremely large neutron absorption cross section for gadolinium. For our GdSe single crystal, the observation of magnetic satellites at reciprocal lattice points $\boldsymbol{G} + \boldsymbol{\tau}$ with $\boldsymbol{\tau} = \{1/2, 1/2, 1/2\}$ is compatible with the antiferromagnetic structure proposed on the basis of the only neutron scattering experiment reported to date [7]. A Néel temperature of 63(1) K is inferred from the temperature variation of the magnetic intensity and there is clear evidence for a discontinuous change in the sample magnetism at 37(1) K. This we suggest corresponds to a transition to the phase II previously observed to occur somewhat below 40 K [8]. The intensity of the $(1/2, 1/2, 7/2)$ reflection decreases suddenly at this temperature but no evidence for new magnetic satellites could be found down to the lower limit of our temperature range at 15 K. The intensity change at 37(1) K will accompany a change in the magnetic domain structure within the single crystal. The reorientation of the ionic spin moments along say [110] would then be favoured in only

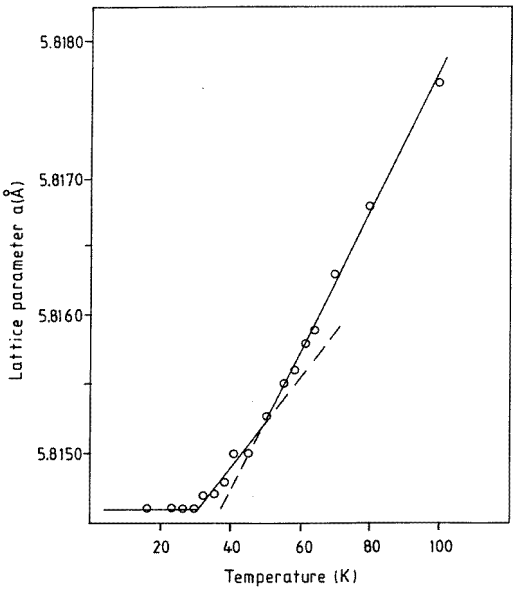

Figure 5. The lattice parameter of GdSe as determined from the (002) and (004) peaks. The lines are guides to the eye and the three regions are discussed in the text.

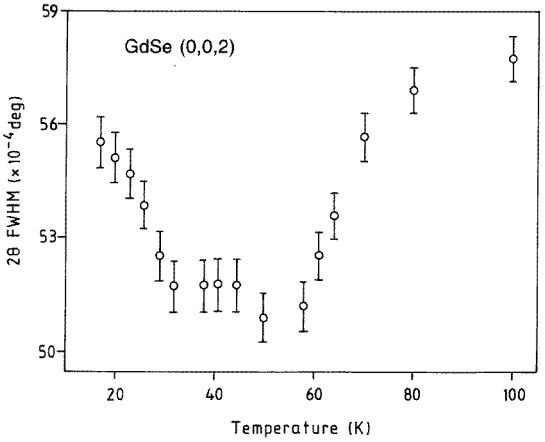

Figure 6. The longitudinal (θ–2θ) width (2θ, FWHM) of the (002) charge peak. The minimum width occurs in the intermediate regime (30–45 K) observed in the data presented in figure 5.

a fraction of these domains which could cause a decrease of the $(1/2, 1/2, 7/2)$ magnetic intensity to a non-zero value. Whereas the neutron magnetic cross section is only sensitive to magnetism components perpendicular to the momentum transfer this is not the case for XRES studies where more subtle geometric considerations apply. The geometry of our experiment does not allow us to relate the observed magnetic intensities to the geometrical term in the cross section involving the spin direction (i.e. $(\varepsilon' \times \varepsilon) \cdot z_n$). This is due to the varying effect of beam attenuation by absorption at the various reflections. We are able, however, to confirm that the magnetic lattice periodicity and structure are indeed of

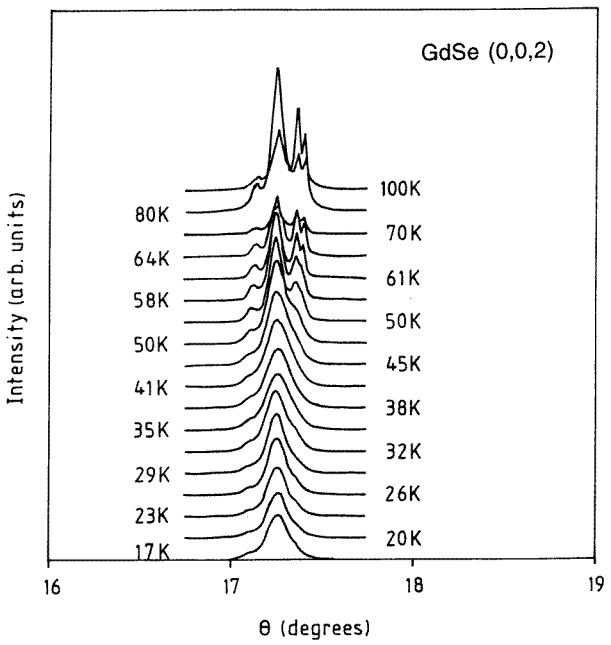

Figure 7. Transverse (θ) scans through the (002) reflection as a function of temperature. Note the broadening with increasing temperature until, at approximately 45 K, several distinct peaks are observed.

the MnO type. We have attempted to characterize the stoichiometry of the sample used as we are conscious that stoichiometry effects play a major role in the observed magnetic properties of these materials. We suggest, therefore, that there would be much to be gained from a systematic series of resonant magnetic x-ray diffraction measurements from samples with slightly differing, and well known, stoichiometries. The resonant technique with its use of characteristic absorption edges unambiguously associates observed magnetic properties with given ionic species in the sample. Additional spectroscopic information may also be present, in that for instance the shape of the resonant enhancement curve can provide information on the electronic structure of the material. In the case of gadolinium we note that the resonant L_{II} and L_{III} enhancements have been found to occur a few electron volts above the absorption edge energies.

Acknowledgments

The authors are grateful to the European Community SCIENCE and Human Capital and Mobility programmes and to the UK Science and Engineering Research Council for financial support and for the award of beam time at the Daresbury Laboratory. We would like to thank D N Furness and S Westland of the Department of Communication and Neuroscience at Keele University and M Reid of Minolta UK for help with the characterization of our single-crystal sample. We are most grateful to O Vogt and the Laboratorium für Festkorperphysik, ETH, Zurich, Switzerland for the loan of the single crystal used in this study.

References

[1] Namikawa K, Ando M, Nakajima T and Kawata H 1985 *J. Phys. Soc. Japan* **54** 4099
[2] Gibbs D, Harshman D R, Isaacs E D, McWhan D B, Mills D and Vettier C 1988 *Phys. Rev. Lett.* **61** 1241
[3] Watson D, Forgan E M, Stirling W G, Nuttall W J and Fort D 1996 *Phys. Rev.* B **53** 726
[4] Hill J P, Vigliante A, Gibbs D, Peng J L and Greene R L 1995 *Phys. Rev.* B **52** 6575
[5] Vettier C, McWhan D B, Gyorgy E M, Kwo J, Buntschuh B M and Batterman B W 1986 *Phys. Rev. Lett.* **56** 757
[6] Detlefs C, Goldman A I, Hill J P, Gibbs D, Stassis C, Canfield P C and Cho B K to be published
[7] McGuire T R, Gambino R J, Pickart S J and Alperin H A 1969 *J. Appl. Phys.* **40** 1009
[8] Hulliger F and Siegrist T 1979 *Z. Phys.* B **35** 81
[9] Hannon J P, Trammel G T, Blume M and Gibbs D 1988 *Phys. Rev. Lett.* **61** 1245
[10] Hill J P and McMorrow D F to be published
[11] Blume M and Gibbs D 1988 *Phys. Rev.* B **37** 1779
[12] Lovesey S 1985 *J. Phys. C: Solid State Phys.* **20** 5625
[13] The interpretation that the $E1$ dipolar term dominates the resonant cross section has been presented several times in the literature. See, e.g., Langridge S, Stirling W G, Lander G H and Rebizant J 1994 *Phys. Rev.* B **49** 12 010
[14] Tang C C, Stirling W G, Lander G H, Gibbs D, Herzog H, Carra P, Thole B T, Mattenberger K and Vogt O 1992 *Phys. Rev.* B **46** 5287
[15] Lovesey S W 1984 *Theory of Neutron Scattering from Condensed Matter* vol 2 (Oxford: Oxford University Press)
[16] Gibbs D, Grübel G, Harshman D R, Isaacs E D, McWhan D B, Mills D and Vettier C 1991 *Phys. Rev.* B **43** 5663
[17] Isaacs E D, McWhan D B, Siddons D P, Hastings J B and Gibbs D 1989 *Phys. Rev.* B **40** 9336
[18] Bohr J, Gibbs D and Huang K 1990 *Phys. Rev.* B **42** 4322
[19] Tang C C, Stirling W G, Jones D L, Wilson C C, Haycock P W, Rollason A J, Thomas A H and Fort D 1992 *J. Magn. Magn. Mater.* **103** 86
[20] Gehring P M, Rebelsky L, Gibbs D and Shirane G 1992 *Phys. Rev.* B **45** 243
[21] Lee S L *et al* 1993 *J. Magn. Magn. Mater.* **127** 145